

Synthesis and electrochemical properties for LiNiO_2 substituted by other elements

K. Kubo ^{*}, M. Fujiwara, S. Yamada, S. Arai, M. Kanda

Materials and Devices Research Laboratory, Toshiba Corporation, 72, Horikawa-cho, Saiwai-ku, Kawasaki 210, Japan

Accepted 24 September 1996

Abstract

$\text{Li}_{1-x}\text{Ni}_{1-y}\text{O}_{2-z}\text{F}_y$ as the cathode materials for rechargeable lithium batteries were synthesized by co-substitution of nickel sites and oxygen sites for LiNiO_2 . The materials were found to possess good properties on charge/discharge cycling without significant deterioration of the initial capacity. In order to investigate the reason the cycle properties were improved, we performed experiments focusing on the crystallographic point of view using X-ray diffractometry accompanied by electrochemical property. These materials were found to restrain none of crystallographic change during charge/discharge regardless of the amount of substitution. According to the charge/discharge curve, the materials indicate relatively low internal impedance. Thus, the main reason for the improvements of the cycle properties may be caused by mechanism which has no direct relation to the above crystallographic change. © 1997 Published by Elsevier Science S.A.

Keywords: Lithium nickelate; Cathode active materials; Fluorine; Lithium secondary batteries; Cobalt substitution; Insertion electrode

1. Introduction

LiNiO_2 is one of the candidates for suitable cathode active materials to realize lithium-ion batteries with high performance. This is the one of the few series having the lithium rechargeable structure with some conductivity of not only ions but also electrons. Furthermore, the materials can be used to realize a battery possessing high energy density, demonstrating a high charging voltage in the 3.5–4.5 V range. However, cycle life has not reached a satisfactory level. Several efforts have been made to improve the charge/discharge cycling properties. The material shows crystallographic change (structural phase transition) during lithium de-intercalation [1,2]. The phase transition may lead to deterioration of the crystal structure. Some research groups performed nickel site substitution by other trivalent cations to restrain the structural phase transition [3–6]. But the exact reason for the decrease of the capacity still remains unknown. Thus, we tried to perform anion site substitution in order to acquire more information about the cycle deterioration.

2. Experimental

We tried fluorine ion substitution into the oxygen site and also lithium ion substitution into the nickel site to keep the

average oxidation number of nickel greater than 3. The relation between composition and oxidation number of the nickel ions is shown in Fig. 1. If it is less than 3, Ni^{2+} ions partly enter into the lithium layer, which may interrupt the motion of the lithium ions leading to the deterioration during the charge and discharge. The open circles in the figure show the samples we ever synthesized. Thus the material series denoted by $\text{Li}_{1+x}\text{Ni}_{1-x}\text{O}_{2-y}\text{F}_y$ ($y < 2x$) were synthesized as follows. The solid-state reaction method was done by heating the mixture with a molar ratio of $(1+x-y):(1-x):y$ for $\text{Li}(\text{OH}) \cdot \text{H}_2\text{O}$, $\text{Ni}(\text{OH})_2$ and LiF , respectively, in an oxygen

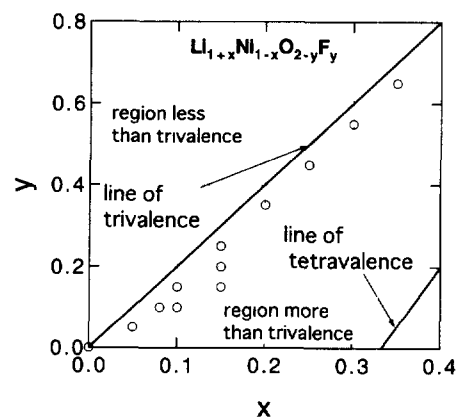


Fig. 1. Relation between the oxidation number of nickel and the composition for $\text{Li}_{1+x}\text{Ni}_{1-x}\text{O}_{2-y}\text{F}_y$. Open circles show samples synthesized compounds.

^{*} Corresponding author. Tel.: 044 (549) 3084; Fax 044 (549) 3391, e-mail. 000093110064@tg.mail.toshiba.co.jp

Table 1

Results of the final composition and the oxidation number of nickel using ICP analysis for lithium, EDTA titration for total nickel, ion chromatography for fluorine and redox titration for the oxidation number of nickel

Nominal composition for $\text{Li}_{1+x}\text{Ni}_{1-y}\text{O}_{2-y}\text{F}_y$	Final Li composition (molar ratio)	Final Ni composition (molar ratio)	Final F composition (molar ratio)	Oxidation number of Ni
$x=0.05, y=0.05$	1.065	0.935	0.044	3.039
$x=0.10, y=0.10$	1.098	0.902	0.084	3.057
$x=0.15, y=0.20$	1.170	0.830	0.170	3.196
$x=0.15, y=0.15$	1.150	0.850	0.112	3.216

gas flow at $\sim 650^\circ\text{C}$ for 50 h. The synthesized samples were ground to obtain a sufficiently fine powder. The crystal structure and phase were identified using the X-ray diffractometer (XRD) with $\text{Cu K}\alpha$. The composition and oxidation number of the nickel ion were measured using a method combined with inductively coupled plasma (ICP) analysis for lithium, ethylenediaminetetraacetic acid (EDTA) titration for total nickel, ion chromatography for fluorine and redox titration for the oxidation number of nickel. As shown in Table 1, the result shows almost no significant difference between the nominal and the final composition. Cathodes were prepared by intimately mixing of the active materials, acetylene black (as the conducting materials) and Teflon binder with the ratio of 80:17:3, then fabricating into the shape of a $1\text{ cm} \times 1\text{ cm}$ sheet. The electrolyte used was a 1 M solution LiClO_4 in the mixed solvent of ethylene carbonate and ethylmethyl carbonate (EC–EMC). A lithium metal anode and a reference electrode were used in this study. Cells for measurements were assembled in a glove box filled with argon gas. In all the measurements, the charge and discharge current was 1 mA and voltage range was from 3 to 4.3 V.

3. Results

Fig. 2 shows the XRD patterns for the $\text{Li}_{1+x}\text{Ni}_{1-y}\text{O}_{2-y}\text{F}_y$, for the range from $(x, y) = (0.0)$ to $(x, y) = (0.35, 0.65)$.

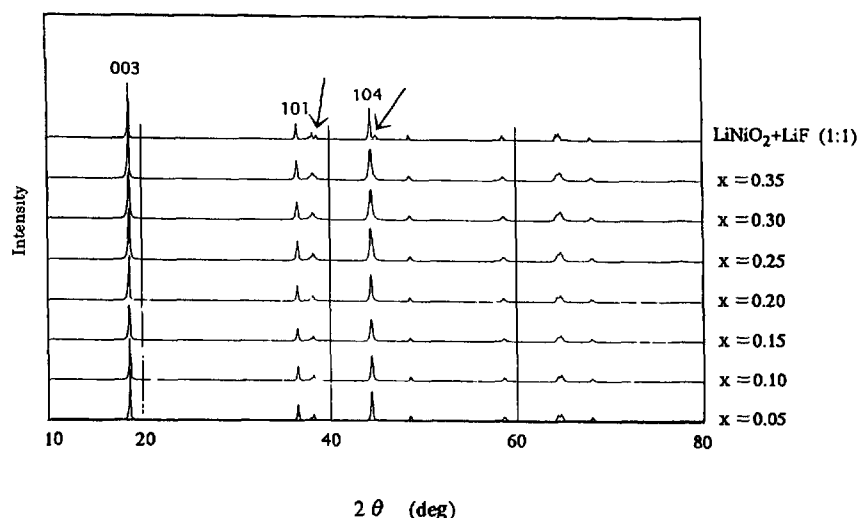


Fig. 2. XRD pattern for $\text{Li}_{1+x}\text{Ni}_{1-y}\text{O}_{2-y}\text{F}_y$ ($y = 2x - 0.05$) ($\text{Cu K}\alpha$). Arrows indicate reflection of LiF.

All samples suggest to be a single phase of the isostructure of LiNiO_2 with an intensity ratio $I(003)/I(104)$ of almost 2, proving that a large difference of the mean scattering factor exists between the lithium and the nickel layer. At the top viewgraph in the figure, we also show the XRD pattern for the mixture of LiNiO_2 and LiF with the molar ratio 1:1, which is the same composition as $\text{Li}_{1.35}\text{Ni}_{0.65}\text{O}_{1.35}\text{F}_{0.65}$ (next to the top viewgraph). The cycling properties for the capacity of $\text{Li}_{1.08}\text{Ni}_{0.92}\text{O}_{1.9}\text{F}_{0.1}$ is shown in Fig. 3 together with that of LiNiO_2 . Though the initial capacity of $\text{Li}_{1.08}\text{Ni}_{0.92}\text{O}_{1.9}\text{F}_{0.1}$ is less than that of LiNiO_2 , during the repetition of cycle, the capacity for the former rises in the first few cycles and shows less deterioration at the higher number of cycles. Thus, it leads to large capacity and long cycle life at the same time. Charge/discharge curves at 1st, 3rd, 5th, 10th and 30th cycle for $\text{Li}_{1.08}\text{Ni}_{0.92}\text{O}_{1.9}\text{F}_{0.1}$ are also shown in Fig. 4. In this viewgraph, enhancement of the capacity in the first few cycles is found to be generated at the final portion of the discharge curve. We have not observed such an interesting phenomena in LiNiO_2 nor other ion substitution. The internal impedance for the active material can be easily estimated by the difference between average charging voltage and average discharging voltage. We calculated the cycle dependence for this difference for $\text{Li}_{1.08}\text{Ni}_{0.92}\text{O}_{1.9}\text{F}_{0.1}$ and LiNiO_2 . While the value for $\text{Li}_{1.08}\text{Ni}_{0.92}\text{O}_{1.9}\text{F}_{0.1}$ is fairly constant after the initial rapid decrease, the value for LiNiO_2 rapidly increases as shown in Fig. 5. The results show that $\text{Li}_{1.08}\text{Ni}_{0.92}\text{O}_{1.9}\text{F}_{0.1}$

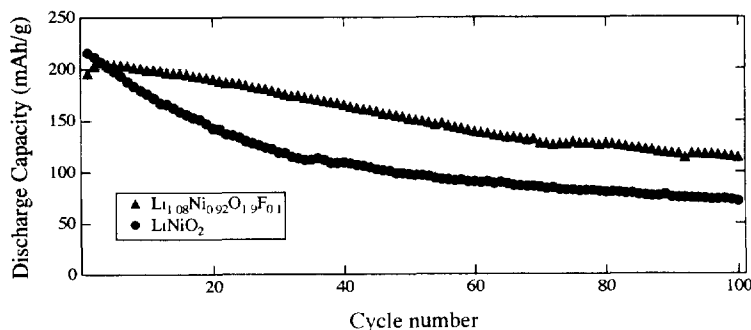


Fig. 3. Discharge properties for $\text{Li}_{1.08}\text{Ni}_{0.92}\text{O}_{1.9}\text{F}_{0.1}$ in 1 M $\text{LiPF}_6/\text{EC}:\text{EMC}$ (1:1), at $I = 1 \text{ mA}$, $V_{\text{max}} = 4.3 \text{ V}$, and $V_{\text{min}} = 3.0 \text{ V}$.

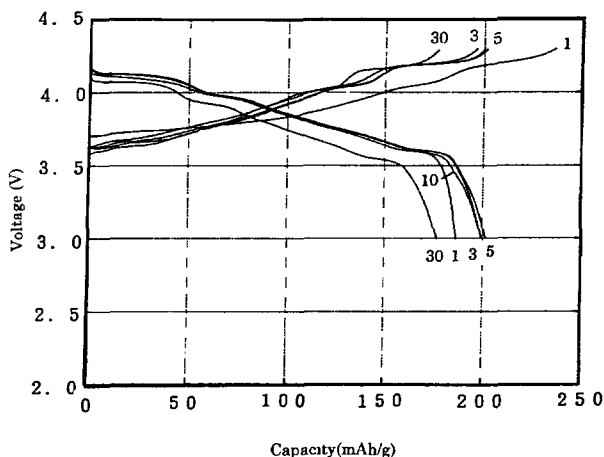


Fig. 4. Charge/discharge characteristics for $\text{Li}_{1.08}\text{Ni}_{0.92}\text{O}_{1.9}\text{F}_{0.1}$ in 1 M $\text{LiPF}_6/\text{EC}:\text{EMC}$ (1:1), at $I = 1 \text{ mA}$, $V_{\text{max}} = 4.3 \text{ V}$, and $V_{\text{min}} = 3.0 \text{ V}$.

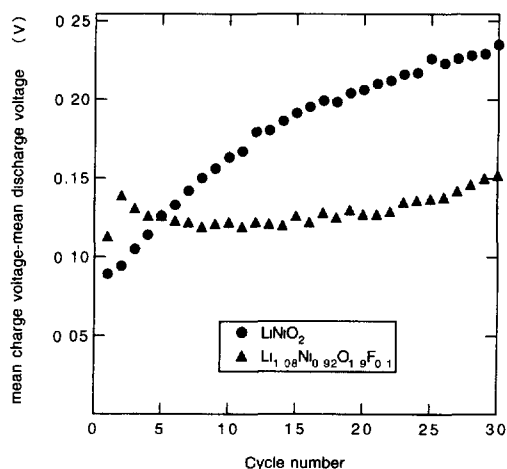


Fig. 5. Variation of the difference between mean voltage of charge and discharge.

does not easily increase its internal impedance due to the charge and discharge. Examinations of XRD pattern versus depth-of-charge for $\text{Li}_{1.1}\text{Ni}_{0.9}\text{O}_{1.85}\text{F}_{0.15}$ were carried out in order to acquire some new information on the mechanism of the crystallographic change. The data were measured during the second charging. All diffraction peak observed were indexed as a hexagonal unit cell. As shown in Fig. 6, during charge the (101) and (104) reflection peaks are split into two peaks shown as solid circles, which can be indexed as

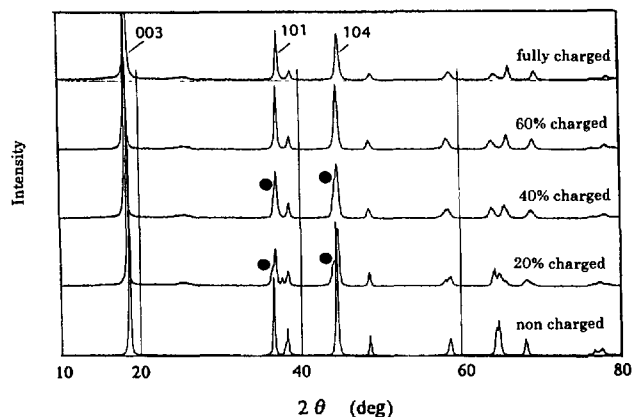


Fig. 6. Variation of XRD pattern for $\text{Li}_{1.15}\text{Ni}_{0.85}\text{O}_{1.75}\text{F}_{0.25}$ during charge ($\text{Cu K}\alpha$). The solid circles indicate slight splitting of peaks for (101) and (104). The depth-of-charge is denoted by the relative ratio to theoretical capacity (237 mAh/g) of the material.

(201) (110) and (202) (111), respectively, based on the hypothesis of a monoclinic unit cell. Despite the fact that the lithium ion is substituted into the nickel site, the results suggest the $\text{Li}_{1.1}\text{Ni}_{0.9}\text{O}_{1.85}\text{F}_{0.15}$ is not like a sample of nickel site substitution by other elements (Al, B, Co, etc.) but is rather closer to non-substituted LiNiO_2 . The fact can be regarded as the lithium ion cannot restrain the crystallographic change, possibly because the binding energy of the monovalent ion with the crystal is weaker than that of the trivalent ion. Though the phase having the unit cell with short c -axis length appeared abruptly around the deepest charge for LiNiO_2 , in $\text{Li}_{1.1}\text{Ni}_{0.9}\text{O}_{1.85}\text{F}_{0.15}$ there is no trace of such a phase. This is one of the clear differences between LiNiO_2 and $\text{Li}_{1.1}\text{Ni}_{0.9}\text{O}_{1.85}\text{F}_{0.15}$. Open-circuit voltage for $\text{Li}_{1.1}\text{Ni}_{0.9}\text{O}_{1.85}\text{F}_{0.15}$ was also measured, as shown in Fig. 7. These data were collected during the second charge; 10 h for each were taken, with no current flow prior to the measurement. This viewgraph shows many step-like structures in the profile. Two plateaus in the profile can be assigned to the aforementioned phase transition. However, we cannot identify the plateau around 4.2 V as coming from any transition because no structural change has been seen in the XRD pattern. Furthermore, other unidentified plateaus also exist. In order to survey the shape of the charge and discharge curve precisely, differential chronopotentiograms for LiNiO_2 and $\text{Li}_{1.08}\text{Ni}_{0.92}\text{O}_{1.9}\text{F}_{0.1}$ were also calculated from the charge and discharge curves. The results

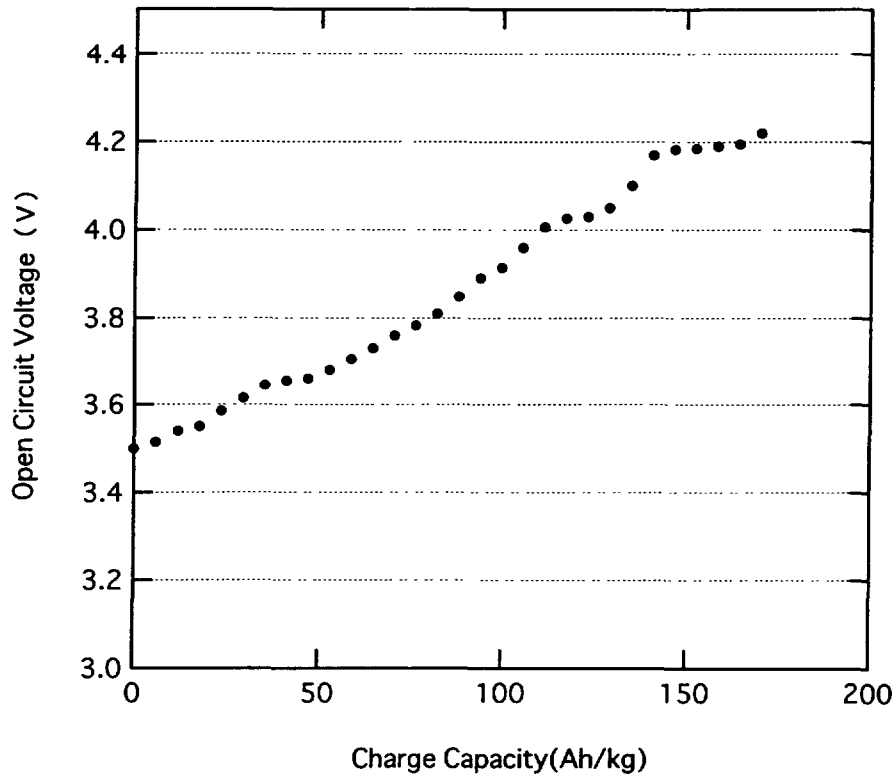


Fig. 7 Open-circuit voltage for $\text{Li}_{1.08}\text{Ni}_{0.92}\text{O}_{1.9}\text{F}_{0.1}$. The electrolyte used was 1 M LiClO_4 in propylene carbonate and dimethoxyethane.

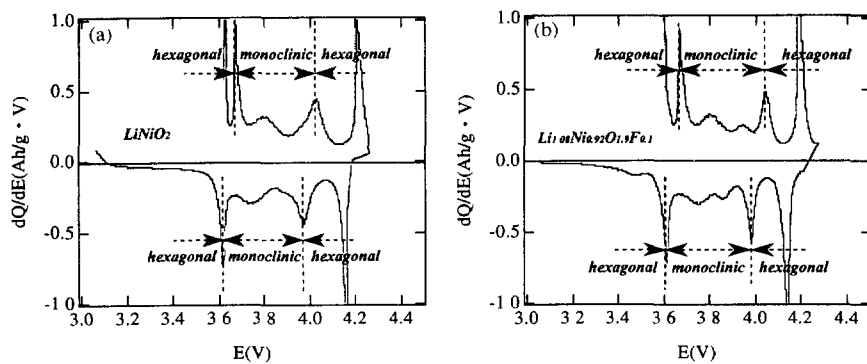


Fig. 8. Differential chronopotentiogram for (a) LiNiO_2 and (b) $\text{Li}_{1.08}\text{Ni}_{0.92}\text{O}_{1.9}\text{F}_{0.1}$.

at the 5th cycle are shown in Fig. 8(a) and (b), respectively. The latter viewgraph has narrower peaks than the former, demonstrating the fact that a more clarified transition for the latter is occurring during the charge and discharge. Another striking feature for the $\text{Li}_{1.08}\text{Ni}_{0.92}\text{O}_{1.9}\text{F}_{0.1}$ is observed. In the monoclinic phase region, two separate peaks are observed, one of which cannot be seen for the LiNiO_2 . This result has been obtained by several groups [1,2]. According to Ohzuku et al. [1], these are solid-state redox peaks whose separation is very sensitive to the slight difference of site occupancy. The $\text{Li}_{1.08}\text{Ni}_{0.92}\text{O}_{1.9}\text{F}_{0.1}$ has better electrochemical properties. Thus if so, the $\text{Li}_{1.08}\text{Ni}_{0.92}\text{O}_{1.9}\text{F}_{0.1}$ may be the sample that can easily yield high quality features using ordinary methods, because in $\text{Li}_{1.08}\text{Ni}_{0.92}\text{O}_{1.9}\text{F}_{0.1}$, the double peaks always appeared in the monoclinic region in the differential chrono-

potentiogram, while we have never been able to synthesize LiNiO_2 indicating a double peak structure.

4. Discussion

One of the interesting features of the results is the rapid increase in capacity and rapid decrease in internal impedance during the first few cycles. The reason may come from the character of the fluorine ions whose weak binding with the lattice gives rise to the position shifting of the fluorine ions and the surrounding ions for the more ideal ones in the crystal lattice during the motion of lithium ions. The more interesting phenomenon is the fact that a relatively long cycle life is observed in the $\text{Li}_{1.08}\text{Ni}_{0.92}\text{O}_{1.9}\text{F}_{0.1}$, while it exhibits the struc-

tural phase transitions, similar to LiNiO_2 except for deep-charged region, but more clearly, during the intercalation and de-intercalation of lithium ions. The fact that more peaks appeared in the monoclinic region during the charge and discharge for $\text{Li}_{1+x}\text{Ni}_{1-y}\text{O}_{2-y}\text{F}_y$ than LiNiO_2 on the differential chronopotentiogram might indicate that the internal stress happened in the material during the charge and discharge is further released by the additional transition. Therefore, we think it may be part of the reason for the life time extension. Another apparent difference between LiNiO_2 and $\text{Li}_{1.08}\text{Ni}_{0.92}\text{O}_{1.9}\text{F}_{0.1}$ is thought to be the fact that the phase with short c -axis length does not exist around the fully charged region. Hence, the possible reason for the enhancement of cycle life for $\text{Li}_{1.08}\text{Ni}_{0.92}\text{O}_{1.9}\text{F}_{0.1}$ is mainly the absence of the abrupt change of the lattice distortion.

5. Summary

$\text{Li}_{1+x}\text{Ni}_{1-y}\text{O}_{2-y}\text{F}_y$ were successfully synthesized in the wide range of $0 < x \leq 0.35$ and $0 < y \leq 0.65$ using solid-state reaction whose nickel site and oxygen site are substituted by lithium and fluorine, respectively. The crystal structure of all the samples is found to be almost the same as that of LiNiO_2 .

According to XRD analysis, interdiffusion of the nickel ions into the lithium layer for all the samples was very slight. The series samples exhibit long cycle life, which may be caused by the absence of the abrupt change of the axis length of the lattice.

Acknowledgements

This work was performed under the financial support of the New Energy and Industrial Technology Development Organization (NEDO) of Japan.

References

- [1] T. Ohzuku, A. Ueda and M. Nagayama, *J. Electrochem. Soc.*, **7** (1993) 1862.
- [2] W. Li, J.N. Reimers and J.R. Dahn, *Solid State Ionics*, **67** (1993) 123.
- [3] T. Ohzuku, A. Ueda and M. Kouguchi, *J. Electrochem. Soc.*, **12** (1995) 4033.
- [4] T. Ohzuku, H. Komori, M. Nagayama, K. Sawai and T. Hirai, *J. Ceram. Soc. Jap.*, **100** (1992) 346.
- [5] T. Ohzuku, J. Kato, K. Sawai and T. Hirai, *J. Electrochem. Soc.*, **138** (1991) 2556.
- [6] M. Fujiwara, S. Yamada and M. Kanda, *Ext. Abstr.*, *34th Battery Symp in Japan, Nagoya, Nov. 1994*, p. 135.